



Population balance for aggregation coupled with morphology changes

Frédéric Gruy

► **To cite this version:**

Frédéric Gruy. Population balance for aggregation coupled with morphology changes. Colloids and Surfaces A: Physicochemical and Engineering Aspects, Elsevier, 2011, 374 ((1-3)), pp.69-76. <10.1016/j.colsurfa.2010.11.010>. <hal-00553189>

HAL Id: hal-00553189

<https://hal.archives-ouvertes.fr/hal-00553189>

Submitted on 6 Jan 2011

HAL is a multi-disciplinary open access archive for the deposit and dissemination of scientific research documents, whether they are published or not. The documents may come from teaching and research institutions in France or abroad, or from public or private research centers.

L'archive ouverte pluridisciplinaire **HAL**, est destinée au dépôt et à la diffusion de documents scientifiques de niveau recherche, publiés ou non, émanant des établissements d'enseignement et de recherche français ou étrangers, des laboratoires publics ou privés.

Population Balance for Aggregation Coupled with Morphology Changes

Frédéric GRUY

Ecole Nationale Supérieure des Mines, 158 Cours Fauriel, 42023 Saint-Etienne,
France, Cedex 2

Corresponding author :

Pr. Frédéric Gruy

Ecole Nationale Supérieure des Mines de Saint-Etienne

gruy@emse.fr

Tel 0033477420202

158 Cours Fauriel, 42023 Saint-Etienne, France, Cedex 2

Abstract

In the past, the kinetics of aggregation has been extensively studied. Aggregation rates were measured and calculated thanks to a population balance. Aggregate morphologies were measured or got by computer simulations. However, the link between the aggregation kinetics and the morphology changes with time is not so clear. The modelling of aggregation may be even more complex as restructuring of aggregates occurs. The aim of this paper is to propose a new formulation taking into account at once kinetics of collision and morphology change rate. We built a bivariate population balance with matter volume and porous volume as internal parameters. The population balance equation contains the standard collision term and a convective term representing the porous volume change. The latter is split into two contributions, which is due to the aggregation process itself and the other one is due to the restructuring. The expressions of the first contribution are determined for Brownian and shear aggregations.

keywords: population balance, bivariate, aggregation, restructuring

1. Introduction

Aggregation of small particles often occurs during industrial processes. The first step of this phenomenon is the collision of particles, which can be due to differential sedimentation, Brownian motion or shear flow in a duct or an agitated vessel. The size of the resulting clusters or aggregates increases with time. However, aggregates become looser and looser and undergo breakage. There is a competition between the cohesive forces inside the aggregate and the shear stress due to the liquid flow. Thus, the final size of aggregates can be calculated from a balance between aggregation and breakage. Aggregation and breakage have been investigated by a lot of researchers. Under certain operating conditions (supersaturation, mass transfer inside the aggregate ...), consolidation or strengthening of aggregates happens. This takes place at the neck between adherent primary particles. The consolidation prevents the breakage of aggregates and leads to more porous clusters than the ones made without consolidation. At the same time, interaction between the flowing liquid and the aggregate can modify the internal structure of aggregates, breakage being the consequence of such a strong interaction. This results in a relative motion of primary particles inside the aggregates and leads to denser aggregates (see, for instance, [1-3]).

The aim of this paper is to propose a new framework to take into account these phenomena. The corresponding modelling will result in a new formulation of the population balance, including aggregation coupled with changes in morphology. The second section of this paper reminds us of any fundamentals on Brownian and shear aggregation. The third section addresses the state of the art about aggregate restructuring and population balance with morphological parameters. The fourth one introduces the new formulation. The fifth one presents the relationship between previous and new formulations. The sixth one gives results for Brownian and shear aggregations and the last one is a discussion about its application.

2. Fundamentals on elementary aggregation processes

Several experimental works and computer simulations show that aggregates have a fractal morphology. In fact, an aggregate containing i identical primary particles of

radius R_i is characterised by: the fractal dimension D_f and the outer diameter R_i . These two parameters are linked by the following relations:

$$R_i = R_1 (i/S)^{1/D_f} \quad (1)$$

The structure factor S is depending on D_f . Its value is close to 1.

Another way to consider fractality uses a continuous variable (volume v) for matter:

$$R \propto v^{1/D_f}$$

In case of a process with only aggregation, i.e. without nucleation and growth, the aggregates are formed from initially non aggregated particles, the mean volume value v_1 of which can be expressed as:

$$v_1 = \Phi / N_1$$

Φ and N_1 are respectively the volume fraction of solid and the number concentration of particles. Then, equation (1) can be written:

$$R_i / R_1 = (v / S v_1)^{1/D_f} \quad (2)$$

With

$$v_1 = 4\pi / 3 R_1^3$$

The main causes of particle collision are the Brownian motion of particles and the local shear in a laminar or a turbulent flow [4]. The aggregation rate between two (i and j) aggregates is characterized by a kinetic constant or kernel $K_{i,j}$.

The Brownian kernel can be approximated by [5, 6]:

$$K_{i,j}^B = K_{i,j}^{B,0} \alpha_{i,j}^B = \frac{2k_B T}{3\mu} (R_i^{-1} + R_j^{-1}) (R_i + R_j) \alpha_{i,j}^B \quad (3a)$$

k_B , T and μ are respectively the Boltzmann constant, the temperature and the fluid dynamic viscosity. $\alpha_{i,j}^B$ is the collision efficiency. In the case of only attractive physical interaction between primary particles, a rough approximation of Eq.(3a) is:

$$K_{i,j}^B = K_{i,j}^{B,0} \alpha^B = \frac{8k_B T}{3\mu} \alpha^B \quad (3b)$$

With α^B having a constant value (≈ 0.5) [7].

The shear aggregation kernel is currently written as:

$$K_{i,j}^S = K_{i,j}^{S,0} \alpha_{i,j}^S = \frac{4}{3} \dot{\gamma} (R_i + R_j)^3 \alpha_{i,j}^S \quad (4a)$$

$\alpha_{i,j}^S$ and $\dot{\gamma}$ are respectively the collision efficiency and the shear rate.

Several relations have been proposed for the collision efficiency. So, in the case of only attractive physical interaction between primary particles, Veerapaneni [5] writes:

$$K_{i,j}^s = \frac{4}{3} \dot{\gamma} \left(\sqrt{\eta_i} R_i + \sqrt{\eta_j} R_j \right)^3 \quad (4b)$$

η_i are the fluid collection efficiency by the aggregate i . From this work, the following approximation can be considered for large porous aggregates:

$$\eta = k \left(R / R_1 \right)^{-(D_f - 1.12)} \quad (5)$$

with $k=0.55$.

Then, equation (4b) can be written:

$$K_{i,j}^s = \frac{\dot{\gamma} v_1 k^{3/2}}{\pi} \left((v_i / S v_1)^{f'} + (v_j / S v_1)^{f'} \right)^3 \quad (6)$$

$$\text{with } f' = 1.56f - 0.5 \quad (7)$$

and $f = 1 / D_f$. f' is smaller than f for standard f values. Brownian and shear flow kernels, that are homogeneous functions of volume, obey:

$$K(\lambda v_i, \lambda v_j) = \lambda^h K(v_i, v_j)$$

with $h=0$ for Brownian kernel and $h=3f'$ for shear aggregation kernel.

3. State of the art

Collision and aggregation lead to an increase of particle size whereas the restructuring decreases the porous volume of the aggregate. Various causes give place to densification: physical forces between primary particles, *e.g.* Van der Waals forces, Brownian motion of the primary particles leading to thermal restructuring, relative motion of the primary particles due to the shear flow, fragmentation-reaggregation steps, *i.e.* fragmentation of a large and loose aggregate followed by aggregation of the two fragments. At our knowledge, the modelling of these phenomena has not yet been performed. However, changes in morphology connected with restructuring have been partially studied by several authors. Their results will be helpful to build a new formulation.

Firstly, we will describe the morphology change of a single aggregate or of a colliding two-aggregate set. Then, we will consider the relationship between morphology change and population balance.

3.1 restructuring laws

* E-mail address: guy@emse.fr

Empirical equations

As a first approximation, clusters keep the same fractal dimension along the aggregation process. However, it follows from some experimental evidence [1-3] that the fractal dimension value increases with time. So, the simplest way for describing this observed increase considers a relaxation law:

$$dD_f / dt = (D_{\max} - D_f) / \tau \quad (8)$$

D_f, D_{\max}, τ are respectively the actual fractal dimension, its maximum value and a relaxation time. The relaxation time includes the above-mentioned physical contributions.

Relaxation time may have a constant value [8], may be a function of the actual aggregate size [9] or may be a function of the mean aggregate size at a given time [10-12].

The relaxation time [9-12] is expressed by means of empirical equations containing fitted parameters. So, 2 or 3 fitted parameters are used for each physical contribution.

These empirical equations well represent the reality, but can be only applied to the considered systems.

Simulations

Starting from assumed restructuring mechanisms at the primary particle scale and being given an initial aggregate morphology, computer simulations lead to the morphology of the aggregate at a given time. As a result, the relaxation time can be deduced. So, in the case of thermal restructuring, Dalis *et al.* [13] show that the relaxation time depends on the temperature, on the size and the number of primary particles in the aggregate:

$$\tau \propto f(i, R_1, T)$$

The computer simulations also give the maximum value of fractal dimension.

Simulation of aggregation has been extensively studied [4]. We will mention the work of Gmachowski [14]. He proposes a new approach of the aggregation modelling by considering an aggregation act for which the fractal dimension can vary along the process. The master equation is the following:

$$(i + j)^{1/D} = \frac{F_1}{F_2} (i^{1/D_i} + j^{1/D_j})$$

$$\text{with } F_k = (1.56 - (1.228 - A_k)^2)^{1/2} - 0.228$$

$$\text{and } A_1 = \frac{D-1}{d-1}, A_2 = \frac{d}{d+D_w-1}$$

$d, D_w, D_i, D(=D_{i+j})$ are respectively the space dimension, the trajectory dimension, the fractal dimension of the aggregate having i primary particles and the one of the resulting aggregate.

The author deduces that:

- cluster-cluster aggregation is such as $D_i = D \quad \forall i$
- cluster-primary particle aggregation [15] is such as the fractal dimension value increases from about 1.75 to 2.5 as the primary particle number increases. Then, the exponent in the mass-size relation is not equal to the standard fractal dimension when $i < 10^6$.
- the fractal dimension can be calculated [16] if the asymptotical population density is assumed as a log-normal function (and by using the maximum entropy principle)
- restructuring may be taken into account [17] by changing the value of F_2 .

Kostoglou and Konstandopoulos [18] use a similar aggregation act for studying Brownian aggregation.

3.2 population balance equation and restructuring

Population balance equation (PBE) is a partial derivative equation, the solution of which is the population density. The latter is a function of the time t and internal parameters for homogeneous suspension. The phenomena acting on the population density are the nucleation, growth, agglomeration and breakage. The corresponding terms are classically included in the PBE. Two ways were proposed in order to take into account aggregate restructuring in the PBE.

3.2.1 1D population balance

More often, the particles are described with only one internal parameter p_1 (for instance, radius R if the particle shape is a sphere). p_1 can be also the volume v or the number of primary particles i in the aggregate if only the aggregation of primary particles is considered. So, the population density for homogeneous suspension depends on t et p_1 : $n(p_1, t)$.

A simple way of considering the restructuring is as follows: if the relaxation time has a constant value or depends on the mean size at a given time, the fractal dimension will be

* E-mail address: gruy@emse.fr

recalculated at each time step by means of Eq. (8) and the new value will be introduced in the aggregation kernel [8,10,11].

Another way due to Baldyga *et al.* [12] is to add a convective term or a growth term

$\frac{\partial Gn}{\partial R}$ into the PBE. The restructuring law appears as:

$$G = dR_i / dt$$

Then,

$$G = -R_i \ln(R_i / R_1) \frac{dD_f}{D_f dt} \quad (9)$$

3.2.2 2D population balance

The 2D PBE contains two internal parameters p_1, p_2 of the aggregate. Thus, the population density is written as $n(p_1, p_2, t)$. These internal parameters can be:

$$p_1 = R, v, i \quad p_2 = a, D_f$$

a is the surface area of the aggregate.

The consolidation, *i.e.* the sintering, of the primary particles inside the aggregate leads to a decrease of the surface area of the aggregate. This can be taken into account (see for instance [19] $p_1 = v \quad p_2 = a$):

$$\frac{\partial n(a, v)}{\partial t} = \frac{\partial n(a, v)}{\partial t} \Big|_{\text{aggregation}} + \frac{\partial n(a, v)}{\partial t} \Big|_{\text{sintering}} \quad (10a)$$

with

$$\frac{\partial n(a, v)}{\partial t} \Big|_{\text{sintering}} = - \frac{\partial G_a n(a, v)}{\partial a} \quad (10b)$$

with the relaxation law for the surface area:

$$G_a = -(a - a_{\min}) / \tau$$

It can be emphasized that the agglomeration term is such as:

$$v_{i+j} = v_i + v_j$$

$$a_{i+j} = a_i + a_j$$

However, the collision integral contains a step function and integration limits that make it more complicated its use and solving.

Likewise, Kostoglou *et al.* [9] propose to use the internal parameters $p_1 = v \quad p_2 = D_f$ in the case of restructuring. Then,

* E-mail address: guy@emse.fr

$$\frac{\partial n(D_f, v)}{\partial t} = \frac{\partial n(D_f, v)}{\partial t} \Big|_{\text{aggregation}} + \frac{\partial n(D_f, v)}{\partial t} \Big|_{\text{restructuring}} \quad (11a)$$

with

$$\frac{\partial n(D_f, v)}{\partial t} \Big|_{\text{restructuring}} = - \frac{\partial G_{D_f} n(D_f, v)}{\partial D_f} \quad (11b)$$

with the relaxation law:

$$G_{D_f} = (D_{\max} - D_f) / \tau(v)$$

Kostoglou and Konstandopoulos [18] consider a 2D PBE including an aggregation act. The PBE is solved by means of a Monte-Carlo simulation. An asymptotical value for D_f is reached after a time depending on the D_f value of the initial aggregates.

4. New formulation

The aim of this paper is to establish a population balance equation by taking into account aggregation and restructuring. The new formalism will permit the introduction of various restructuring mechanisms in a simple way. The framework will be a bidimensional population balance. The two internal parameters will be chosen so that the additivity is respected along the aggregation process. We selected the matter volume v (or the number of primary particles) and the pore volume vp . Thus, $v+vp$ is the volume of the aggregate. The pore volume is preferred to the porosity because the latter is not an additive property along the aggregation process. Aggregation without and with restructuring will be treated by means of the same formalism.

4.1 aggregation without restructuring

Aggregation process is split into two successive steps (Figure 1):

- Collision between two aggregates leading to a new particle composed in the two aggregates in contact. This step can be written as:

$$(v_i, vp_i) + (v_j, vp_j) \rightarrow (v_i + v_j, vp_i + vp_j) \quad (12)$$

This step appears in the population balance equation as a standard collision term.

The kernel is the aggregation kernel $K^0(v_i, vp_i, v_j, vp_j) = K_{i,j}^0(v_i + vp_i, v_j + vp_j)$.

For instance, the corresponding expression for a Brownian aggregation is:

$$K^0(v_i, vp_i, v_j, vp_j) = \frac{2kT}{3\mu} \left[(v_i + vp_i)^{1/3} + (v_j + vp_j)^{1/3} \right] \left[(v_i + vp_i)^{-1/3} + (v_j + vp_j)^{-1/3} \right] \quad (13a)$$

and for a shear aggregation

$$K^0(v_i, vp_i, v_j, vp_j) = \frac{\dot{\gamma}}{\pi} \left[(v_i + vp_i)^{1/3} + (v_j + vp_j)^{1/3} \right]^3 \quad (13b)$$

- Overlapping of the two initial aggregates and restructuring of the new particle. In the case of fractal aggregates with constant fractal dimension, the new particle will have a bigger volume than the sum of the initial ones. Thus, this stage corresponds to an expansion. This step will be modeled by using a convective or growth term:

$$-\frac{\partial G_{vp}^0 n(vp, v)}{\partial vp} \quad (13c)$$

G_{vp}^0 is a function of vp and probably of v . G_{vp}^0 represents the expansion rate of the two initial aggregates set. This convective term can be considered as a virtual restructuring. This modelling introduces no additional assumption such as fractal morphology, *i.e.* relationship between pore volume and matter volume.

Asymptotic behaviour

The aggregation kernels (for instance, Brownian or shear aggregation, Eqs. (3b), (4b)) are homogeneous functions of the sizes of colliding particles. If the expansion rate is also an homogeneous function of vp and v , e.g. $G_{vp}^0 \propto vp^m$ or $G_{vp}^0 \propto (v + vp)^m$, we can write:

$$K_{x,y}^0(\lambda x, \lambda y) = \lambda^p K_{x,y}^0(x, y)$$

$$G_{vp}^0(\lambda x) = \lambda^m G_{vp}^0(x) \text{ or } G_{vp}^0(\lambda x, \lambda y) = \lambda^m G_{vp}^0(x, y)$$

It has been proved that large aggregates have a fractal-like morphology for long time:

$$t \rightarrow \infty \quad vp \propto v^{3/D_f}$$

Thus, we observe an asymptotical behaviour, as self-similarity:

$$t \rightarrow \infty \quad vp \propto v^{3/D_f} \quad n(v, vp, t) \rightarrow n_\infty(v, t) \rightarrow t^\beta g(vt^\alpha)$$

The use of these relations into the PBE [20] leads to:

$$m = 1 - D_f / 3 \text{ for Brownian aggregation} \quad (14a)$$

$$m = 2 - D_f / 3 \text{ for shear aggregation } (f=f') \quad (14b)$$

4.2 aggregation with restructuring

* E-mail address: guy@emse.fr

Restructuring will be taken into account by means of the overall convective term:

$$G_{vp} = G_{vp}^0 + G_{vp}^1 \quad (15)$$

where G_{vp}^1 is the restructuring (contraction) rate and G_{vp}^0 is the expansion rate introduced by modelling of aggregation. An approximate expression for G_{vp}^1 could be written:

$$G_{vp}^1 = -K_R v (vp/v)^p \quad (16)$$

The p ($p > 0$) exponent depends on the contraction mechanism. The kinetic constant K_R has to consider the competition between contraction and consolidation, the latter annoying the former. As already used for drop coalescence [21], the kinetic constant K_R could be expressed as:

$$K_R = K_{R,\max} / (1 + \tau_1 / \tau_2) \quad (17)$$

τ_1, τ_2 respectively represent the characteristic times for « free of sintering » contraction and consolidation.

5. Comparison between old and new formulations

Two aspects characterize the aggregation: the kinetics of the collision and the topology of the aggregates. The classical formulation considers them independent to each other. The topology of aggregates is observed (for instance, by SEM) or got by computer simulations. Moreover, topology is obtained after long time aggregation. On the other hand, the kinetic rate is measured or modeled by means of a population balance.

The new formulation considers at the same time kinetics and topology by means of the expansion rate. Then, one searches the aggregation kernel $K'(v_i, vp_i, v_j, vp_j)$ and the expansion rate G_{vp}^0 leading to the same aggregation dynamics and topology than the ones obtained by the classical formulation.

The classical formulation uses the 1D population balance equation:

$$\frac{\partial n}{\partial t} = \frac{1}{2} \int_0^v K(\tilde{v}, v - \tilde{v}) n(\tilde{v}) n(v - \tilde{v}) d\tilde{v} - n(v) \int_0^\infty K(v, \tilde{v}) n(\tilde{v}) d\tilde{v} \quad (18)$$

with $K(v, \tilde{v}) = K^0(v, vp, \tilde{v}, \tilde{v}p) \alpha_0$ and $vp = g(v)$ for $t \rightarrow \infty$

$$\text{for instance, } \left(\frac{v + vp}{v_1} \right)^{1/3} = \left(\frac{v}{Sv_1} \right)^{1/Df} \quad (19a)$$

or

$$v + vp \approx vp \approx g(v) = v_1 \left(\frac{v}{Sv_1} \right)^{3/Df} \quad (19b)$$

The new formulation uses the 2D population balance equation:

$$\begin{aligned} \frac{\partial n'}{\partial t} + \frac{\partial G_{vp}^0(v, vp) n'}{\partial vp} = \\ \frac{1}{2} \int_0^v \int_0^{vp} K'(\tilde{v}, \tilde{vp}, v - \tilde{v}, vp - \tilde{vp}) n'(\tilde{v}, \tilde{vp}) n'(v - \tilde{v}, vp - \tilde{vp}) d\tilde{v} d\tilde{vp} \\ - n'(v, vp) \int_0^\infty \int_0^\infty K'(v, vp, \tilde{v}, \tilde{vp}) n'(\tilde{v}, \tilde{vp}) d\tilde{v} d\tilde{vp} \end{aligned} \quad (20)$$

$$\text{with } K'(v, vp, \tilde{v}, \tilde{vp}) = K^0(v, vp, \tilde{v}, \tilde{vp}) \alpha_1$$

Thus, the problem to solve is the following:

Which are the expressions of $G_{vp}^0(v, vp)$ and K' , such as (18) \equiv (20) and ($vp = g(v)$)?

The relation between the 2D and 1D population densities ($t \rightarrow \infty$) is:

$$n'(v, vp) = n(v) \delta(vp - g(v))$$

$$\text{and } n'(v - \tilde{v}, vp - \tilde{vp}) = n(v - \tilde{v}) \delta(vp - \tilde{vp} - g(v - \tilde{v}))$$

$n(v)$ is the solution of Eq.(18).

By using a moment method and by applying to Eq.(20) the operator O defined by

$$O(f) = \int_0^\infty f vp^p dv, \text{ one obtains:}$$

$$\begin{aligned} \frac{\partial n(v)}{\partial t} - pn(v) g^{-1}(v) G_{vp}^0(g(v)) = \\ \frac{g^{-p}(v)}{2} \int_0^v K'(\tilde{v}, g(\tilde{v}), v - \tilde{v}, g(v - \tilde{v})) [g(\tilde{v}) + g(v - \tilde{v})]^p n(\tilde{v}) n(v - \tilde{v}) d\tilde{v} \\ - n(v) \int_0^\infty K'(v, g(v), \tilde{v}, g(\tilde{v})) n(\tilde{v}) d\tilde{v} \quad p \geq 0 \end{aligned} \quad (21)$$

for $p=0$:

$$\begin{aligned} \frac{\partial n(v)}{\partial t} = & \\ \frac{1}{2} \int_0^v K'(\tilde{v}, g(\tilde{v}), v-\tilde{v}, g(v-\tilde{v})) n(\tilde{v}) n(v-\tilde{v}) d\tilde{v} & \\ - n(v) \int_0^\infty K'(v, g(v), \tilde{v}, g(\tilde{v})) n(\tilde{v}) d\tilde{v} & \end{aligned}$$

Eqs.(18) and (20) are equivalent if:

$$K'(v, g(v), \tilde{v}, g(\tilde{v})) = K(v, \tilde{v}) \quad (22)$$

By subtracting Eq.(21) (with p=0) at Eq.(21) (with p=1):

$$G_{vp}^0(g(v)) = \frac{1}{2} \int_0^v K(\tilde{v}, v-\tilde{v}) [g(v) - g(\tilde{v}) - g(v-\tilde{v})] \frac{n(\tilde{v})n(v-\tilde{v})}{n(v)} d\tilde{v} \quad (23)$$

Eq.(23) calls for several remarks:

- i.** The method leading to Eq. (23) belongs to a mean field theory.
- ii.** If $g(v) - g(\tilde{v}) - g(v-\tilde{v}) = 0$, then $G_{vp}^0(vp) = 0$: As expected, an aggregation step without porous volume change needs no G_{vp}^0 .
- iii.** If $g(v)$ obeys a power law as $vp = g(v) \propto v^{3/D_f}$ with an exponent $3/D_f$ bigger than 1, then $\Delta g = g(v) - g(\tilde{v}) - g(v-\tilde{v}) > 0 \quad \forall v$ and $G_{vp}^0(vp) > 0$. Thus, aggregation proceeds with expansion or porous volume increase.
- iv.** Only zero and first order moments of the 2D population density were used in order to establish Eq.(23) because the higher order moments ($p \geq 2$) are not undoubtedly bounded. By contrast, the first order moment obeys the inequality: $\int_0^\infty n(v, vp) vp dv p < \int_0^\infty dv \int_0^\infty n(v, vp) vp dv p < 1$ (i.e, the pore volume fraction is smaller than 1).
- v.** The new formulation contains two successive steps (collision and expansion): K' is the kinetic constant of the collision rate and G_{vp}^0 is the expansion rate. As K , in the classical formulation, includes the two steps at the same time, the inequality $K' > K$ should be verified, contrary to the previous result ($K' = K$). This possible discrepancy is due to the final aggregate volume (i.e., the arguments in the kernels K and K') considered in each formulation. The following proof can be done:

Starting from

$$K'(v, g(v), \tilde{v}, g(\tilde{v})) = K(v, \tilde{v}) = F_1(\tilde{v} + g(\tilde{v}), v + g(v))$$

where v is the final volume. Then,

$$\begin{aligned} K'(\tilde{v}, g(\tilde{v}), v, g(v)) &= F_2(\tilde{v} + g(\tilde{v}), v + g(\tilde{v}) + g(v - \tilde{v})) \\ &= F_1(\tilde{v} + g(\tilde{v}), v + g(v)) = F_1(\tilde{v} + g(\tilde{v}), v + g(\tilde{v}) + g(v - \tilde{v}) + \Delta g) \\ &\Rightarrow \\ K'(\tilde{v}, g(\tilde{v}), v - \tilde{v}, g(v - \tilde{v})) &= F_1(\tilde{v} + g(\tilde{v}), v - \tilde{v} + g(v - \tilde{v}) + \Delta g) \end{aligned} \quad (24)$$

By taking a first-order Taylor series of F_I (F_I is replaced by K) and a symmetrisation for the volume:

$$K'(x, y) \simeq K(x, y) + \frac{\Delta g}{2} \left(\frac{\partial K}{\partial x} + \frac{\partial K}{\partial y} \right)$$

x et y are the overall (pore and matter) volumes of colliding aggregates.

As a consequence, if the argument values (x and y) are identical, $K' > K$.

Moreover, a physical reason has to be mentioned for $K' > K$: as the first step leads to a very loose aggregate, the hydrodynamic resistance and the physical forces during its formation are very weak. Thus, the collision efficiency of the first step, and then the aggregation kernel, is higher than the one of the classical formulation.

As Eq.(24) is difficult to apply, we will use the kernels (Eqs.(13a-b), *i.e.* $\alpha_1 = 1$) corresponding to the physical characteristics of step 1.

The next section presents an estimate of the expansion rate G_{vp}^0 (Eq. (23)) for Brownian and shear aggregation.

6. Calculation of the expansion rate

6.1. Brownian aggregation

The Brownian kernel is chosen as a constant:

$$K_0 \simeq K^{B,0} \quad \alpha_0 \simeq \alpha^{B,0}$$

The number concentration N_j for aggregates with j primary particles obeys the relation [22]:

$$N_j = N_{10} (t')^{j-1} (1+t')^{-j-1}$$

$t' = t/t_c$ is the dimensionless time. N_{10} and $t_c = 2/(K_0 \alpha_0 N_{10})$ are respectively the initial number concentration in primary particles and the characteristic time for Brownian

* E-mail address: guy@emse.fr

aggregation. But, the number concentrations for Brownian aggregation have the interesting property, denoted P1:

$$N_{i-j}N_j = N_{10}N_i f(t') \quad \text{P1} \quad (25)$$

With continuous variables, the population density can be written as:

$$n(v) = \frac{N_{10}}{v_1} (t')^{(v/v_1)-1} (1+t')^{-(v/v_1)-1} \quad (26)$$

and

$$n(v) = n(\tilde{v})n(v-\tilde{v})\frac{v_1}{N_{10}}t'(1+t')$$

By using Eqs 23, 19b and property P1, one gets the expression:

$$G_{vp}^0(v) = \frac{K_0 N_{10}}{2t'(1+t')} S^{-3/D_f} v_1 \frac{3-D_f}{3+D_f} (v/v_1)^{1+3/D_f} \quad (27)$$

For long time ($t/t_c \gg 1$), this expression can be transformed into:

$$\frac{d(vp/v_1)}{dt'} = \frac{9(3+D_f)\alpha_0}{SD_f^2(3-D_f)} ((v+vp)/v_1)^{1-D_f/3} \quad (28)$$

The asymptotic behaviour with the exponent $1-D_f/3$ is verified.

The fractal dimension for Brownian aggregation without restructuring is equal to 1.8 ($S=0.54$). This value is coming from computer simulations. Thus,

$$G_{vp}^0'(vp/v_1) = \frac{d(vp/v_1)}{dt'} = 10.25((v+vp)/v_1)^{0.4} \quad (29)$$

6.2 shear aggregation

The general expression of the aggregation kernel is that of Veerapaneni (Eq.(6)).

Thus, two exponents will be introduced: one f for the fractal geometry of aggregates and another one f' for the kinetic constant:

$$vp = g(v) = v_1 \left(\frac{v}{v_1 S} \right)^{3f} = Dv^{3f}$$

$$K(v, \tilde{v}) = B(v^{f'} + \tilde{v}^{f'})^3$$

with

$$B = \frac{\dot{\gamma} v_1 k^{3/2}}{\pi} (Sv_1)^{-3f'}$$

The population density for shear aggregation has no property such as P1. Then, the exact solution of 1D population balance will be replaced by an approximate function having the property P1':

$$n(\tilde{v}, t)n(v - \tilde{v}, t) = n(v, t)A(t)h(\tilde{v}, v - \tilde{v}) \quad (30)$$

h is a homogeneous function.

The Gamma function, which is widely used for approximating experimental particle size distributions, has such a property P1' [23]:

$$n(v, t) = Av^{\mu-1}e^{-\mu v/\bar{v}} \quad (31)$$

\bar{v}, σ are the mean value and the standard deviation, while $\mu = (\bar{v}/\sigma)^2$. These quantities can be expressed from the distribution moments M_j , that depend on the time:

$$\bar{v} = M_1 / M_0$$

$$\sigma = \bar{v} \sqrt{\frac{M_0 M_2}{M_1^2} - 1}$$

A is a normalization constant:

$$\int_0^{\infty} n(v, t) v dv = \Phi \quad (\Rightarrow A = \Phi \left(\frac{\mu}{v} \right)^{\mu+1} / \Gamma(\mu+1))$$

thus

$$G_{vp}^0(g(v)) = \frac{1}{2} \int_0^v K(\tilde{v}, v - \tilde{v}) [g(v) - g(\tilde{v}) - g(v - \tilde{v})] \left[\frac{\tilde{v}(v - \tilde{v})}{v} \right]^{\mu-1} A(t) d\tilde{v} \quad (32)$$

Thus, the calculation of G_{vp}^0 necessitates the three moments M_0, M_1 and M_2 . In the case of shear aggregation without fragmentation, the moments obey:

$$\frac{dM_j}{dt} = \frac{B}{2} \int_0^{\infty} \int_0^{\infty} [(v + \tilde{v})^j - v^j - \tilde{v}^j] [v^{f'} + \tilde{v}^{f'}]^3 n(v, t)n(\tilde{v}, t) dv d\tilde{v} \quad (33)$$

Following Park and Lee [24-26] and Gruy [27], the three first moments, the mean value and the standard deviation can be calculated thanks to the ordinary differential equation (ODE) system:

$$\frac{d\beta_1}{dt'} = (1 - 3f') \beta_2^{-3f'/2} F(\beta_2) \quad (34a)$$

$$\beta_1 \frac{d\beta_2}{dt'} + \frac{\beta_2}{1 - 3f'} \frac{d\beta_1}{dt'} = 2\beta_2^{3f'/2} F(\beta_2) \quad (34b)$$

$$F(\beta_2) = \beta_2^{\frac{9}{2}f'^2} (1 + 3\beta_2^{-2f'^2}) \quad (34c)$$

with

* E-mail address: groy@emse.fr

$$\beta_1 = \left(\bar{v}/v_1\right)^{1-3f'}, \beta_2 = \frac{\sigma^2}{v} + 1, t' = t/t_c \text{ and } t_c = \frac{\pi S^{3f'}}{\gamma \Phi k^{3/2}}$$

by taking the initial conditions:

$$\beta_1 = 1 \text{ and } \beta_2 = 1 + \varepsilon$$

$\beta_2(t)$ tends asymptotically towards constant values depending on f' . The asymptotical values $\beta_{2,a}$ are not dependent on the initial β_2 values. However, if the exponent $3f'$ is

higher than 1, gelation occurs, i.e. divergence of the ODE system (or the standard deviation). This asymptotical behaviour corresponds to the following values for β_2 and

$d\beta_1/dt'$:

$$\beta_{2,a} = 2^{1/(1-3f')} \quad (35)$$

$$d\beta_{1,a}/dt' = C = (1-3f') \left[2^{-3f'/2} + 3 \times 2^{-f'(3-5f')/(1-3f')/2} \right] \quad (36)$$

Let us apply these results to Eq.(32) in order to obtain G_{vp}^0 :

$$G_{vp}^0(g(v)) = \Phi D B C^{-(1+\mu)/(1-3f')} t'^{-(1+\mu)/(1-3f')} \mu^{\mu+1} \Gamma^{-1}(\mu+1) v_1^{-(1+\mu)} v^{\mu+6f'} F(f, f') \quad (37a)$$

with

$$F(f, f') = \frac{1}{2} \int_0^1 \left(x^f + (1-x)^f \right)^3 \left[1 - x^{3f} - (1-x)^{3f} \right] \left[x(1-x) \right]^{\mu-1} dx \quad (37b)$$

Moreover,

$$G_{vp}^0(g(v)) = dvp/dt = v_1 t_c^{-1} d(vp/v_1)/dt' = v_1 t_c^{-1} G_{vp}^0 \quad (38)$$

Thus,

$$G_{vp}^0(g(v)/v_1) = E(f, f') (g(v)/v_1)^{(\mu+6f)/(3f)} t'^{-(1+\mu)/(1-3f')} \quad (39a)$$

with

$$E(f, f') = C^{-(1+\mu)/(1-3f')} \mu^{\mu+1} \Gamma^{-1}(\mu+1) S^{\mu+3f'} k^{-3/2} F(f, f') \quad (39b)$$

Finally,

$$G_{vp}^0(vp/v_1) = H(f, f') ((v+vp)/v_1)^{ex} \quad (40a)$$

with

$$H(f, f') = \frac{3f}{1-3f'} \frac{\mu+3f'}{\mu+3f'} \left(E \frac{1-3f'}{3f} \frac{\mu+3f'}{\mu+3f'} \right)^{(3f'-1)/(3f'+\mu)} \quad (40b)$$

and

$$ex = 1 - \frac{1-3f'}{3f} \frac{\mu+3f'}{\mu+3f'} \quad (40c)$$

If $f'=f$, the asymptotic behaviour with the exponent $2 - D_f/3$ is verified.

The figure 2a represents the function $H(f, f')$ (Eq. (40b)). We note that the effect of f on G_{vp}^0 is weaker than the one of f' . The figure 2b represents the exponent ex of the power law (Eq. (40c)) versus D_f .

Following Torres [28], simulations of shear aggregation lead to a fractal dimension ($D_f=1/f$) equal to 1.8, while Potanin [29] suggests the value 1.98. We will take the intermediate value 1.9.

From Eqs (7), (35-36), (40a-c), one deduces:

$$G_{vp}^0 (vp/v_1) = 1.5 \left((v + vp)/v_1 \right)^{0.97} \quad (41)$$

7. Discussion

The new formulation has been applied in the case of Brownian aggregation for which experiments, calculations and computer simulations were achieved by other investigators. Monte Carlo Simulations (MCS) have been performed to solve the particle dynamics equation for coagulation of particles undergoing morphology changes (Eqs. 20 and 29). Here we use the algorithm suggested by Tandon and Rosner [19] when they studied aggregation coupled with surface area reduction. In our case, the sintering kinetic law was replaced by the porous volume expansion law (Eq. 29). The aggregation kernel has been taken as a constant. The choice of the time step in the MCS needs a particular consideration. As a consequence we used the method proposed by Smith and Matsoukas [30] in which the number of particles is kept constant. To start the simulations we consider a set of N ($N=5000$) particles, each of unit volume and porous volume equal to 0. During aggregation each aggregate is characterized by v and vp . One deduces its fractal dimension by means of Eq. 19a.

From these simulations we show that:

- At the beginning of aggregation small and very porous aggregates are present and may survive. This is due to the convective term (Eq.13c), that allows certain aggregates to increase their porous volume whereas the other aggregates collide each other. The growth of the porous volume stops when the aggregate disappears due to collision. Certain small aggregates, waiting for the collision, get a higher porosity. However, their amount is smaller than 1%.
- All the small aggregates ($i>20$) have the same behaviour. Let us consider aggregates with a given number of primary particles (for instance $i=50$). They suddenly appear and their fractal dimension value is in the range [1.9-2.0]. Their

number rapidly increases, then it slowly decreases (figure 3). Whatever the time the fractal dimension distribution of these aggregates is narrow. The standard deviation of the distribution is about 0.04. During the aggregation the mean fractal dimension decreases. The value corresponding to the maximum number of aggregates ($i=50$) is 1.65.

- After a long time, the small aggregates disappear. The fractal dimension distribution is within the range [1.6-1.8] and the mean fractal dimension tends to the value 1.80 (figure 4). The distribution is skewed with a tail for the smallest values ($Df < 1.7$).

These results have been compared to previous works. A controversy concerns the morphology of small aggregates. Adachi et al. [31] have studied the DLCA mechanism. They observe an increase of the fractal dimension from 1 for very small aggregates ($i < 5$) to 1.75-1.80 for aggregates with $i > 50$. Yang and Biswas [32] did the same observation. Lattuada et al [33] built aggregates by simulation and showed that the aggregates are fractal-like if $i > 20$. Our MCS of aggregation dynamics are partially in agreement with the results of these investigators. We observe small aggregates with low Df value and a change of Df with time which is the same for the aggregates with $i > 20$. However, in our modelling, the morphology is a dynamic property; the Df value of aggregates is close to 1.8 during their formation (see figure 3), but it becomes smaller along their removal due to collisions.

All the aggregates contain a large number of primary particles after a long time. The fractal dimension distribution varies very slowly whereas matter volume distribution tends to an asymptotic shape [19]. This result was expected because of the way for calculating the expansion rate.

8. Summary and conclusion

The morphology changes are taken into account thanks to a 2D population balance, the internal variables of which are the volume of matter and the porous volume of the aggregate. The mechanism of aggregation is split up in two steps: the collision itself characterized by the collision kernel without collision efficiency (Eqs.(13a-b)) and the change of the porous volume of the aggregate (Eq.(15)). The latter contains a contribution due to the porous volume increase occurring for all aggregation processes and another one due to the restructuring itself. The bivariate population balance

equation is solved with the corresponding initial conditions and boundary conditions.

The latter are:

$$n(v, vp, t) = 0 \quad (42a)$$

for

$$vp = v_1 \left(\frac{v}{Sv_1} \right)^3 - v \quad (42b)$$

$$n(v, vp, t) = 0 \quad (43a)$$

for

$$vp = \frac{1 - Cp}{Cp} v \quad (43b)$$

Cp is the maximum compactness of the aggregate. Eqs (42b) and (43b) define on a (v, vp) diagram two lines which are the boundaries of the integration domain.

As the contribution of the aggregation process to the porous volume change was established in this paper (Eqs. (29) and (41)) for two important aggregation mechanisms, the one of the restructuring has to be determined as the term G_{vp}^1 . This task is in progress.

Acknowledgments

We acknowledge the Agence Nationale de la Recherche for support of this research.

References

- [1] S. di Stasio, "Observation of restructuring of nanoparticle soot aggregates in a diffusion flame by static light scattering", *J. Aerosol Sci.*, 32(2001)509
- [2] Y. Adachi, K. Aoki, "Restructuring of small flocs of polystyrene latex with polyelectrolyte", *Colloids and Surfaces A: Physico-chemical and Engineering Aspects*, 342(2009)24
- [3] J. Yu, D. Wang, X. Ge, M. Yan, M. Yang, "Flocculation of kaolin particles by two typical polyelectrolytes: A comparative study on the kinetics and floc structures", *Colloids and Surfaces A : Physico-chemical and Engineering Aspects*, 290(2006)288
- [4] M. Elimelech, J. Gregory, X. Jia, R. Williams, *Particle deposition and aggregation, measurement, modelling and simulation*, Butterworth-Heinemann Ltd, Oxford, 1995.

- [5] S. Veerapaneni, M.R. Wiesner, “Hydrodynamics of fractal aggregates with radially varying permeability”, *J. Coll. Interf. Sci.* 177(1996)45
- [6] L. Gmachowski, “ Hydrodynamics of aggregated media”, *J. Coll. Interf. Sci.*, 178(1996)80
- [7] A.S. Kyriakidis, S.G.Yiantsios, and A.J. Karabelas, “A study of colloidal particle Brownian aggregation by light scattering techniques”, *J. Coll. Interf. Sci.*, 195(1997)299
- [8] M. Soos, J. Sefcik, M. Morbidelli, “Investigation of aggregation, breakage and restructuring kinetics of colloidal dispersions in turbulent flows by population balance modelling and static light scattering”, *Chem. Eng. Sci.*, 61(2006)2349
- [9] M. Kostoglou, A.G. Konstandopoulos, S.K. Friedlander, “Bivariate population dynamics simulation of fractal aerosol aggregate coagulation and restructuring”, *Aerosol Sci.* 37(2006)1102
- [10] C. Selomulya, R. Amal, G. Bushell, T.D. Waite, “Evidence of shear rate dependence on restructuring and breakup of latex aggregates”, *J. Coll. Interf. Sci.*, 236(2001)67
- [11] C. Selomulya, G. Bushell, R. Amal, T.D. Waite, “Understanding the role of restructuring in flocculation: The application of a population balance model”, *Chem. Eng. Sci.*, 58(2003)327
- [12] J. Baldyga, W. Orciuch, L. Makowski, M. Malski-Brodzicki, K. Malik, “Break up of nano-particle clusters in high-shear devices”, *Chem. Eng. Progress*, 46(2007)851
- [13] A. Dalis, S.K. Friedlander, “ A lattice chain model for the thermal restructuring of nanoparticle chain aggregates”, *Aerosol Sci.* 36(2005)27
- [14] L. Gmachowski, “Estimation of the dynamic size of fractal aggregates”, *Colloids and surfaces, A: Physicochemical and Engineering Aspects* 170(2000)209
- [15] L. Gmachowski, “Calculation of the fractal dimension of aggregates”, *Colloids and surfaces, A: Physicochemical and Engineering Aspects* 211(2002)197
- [16] L. Gmachowski, “A method of maximum entropy modelling the aggregation kinetics” *Colloids and surfaces, A: Physicochemical and Engineering Aspects* 176(2001)151
- [17] L. Gmachowski, “Aggregate restructuring and its effect on the aggregate size distribution”, *Colloids and surfaces, A: Physicochemical and Engineering Aspects* 207(2002)271
- [18] M. Kostoglou, A.G. Konstandopoulos, “Evolution of aggregate size and fractal dimension during Brownian coagulation”, *Aerosol Sci.* 32(2001)1399

- [19] P. Tandon, D.E. Rosner, "Monte Carlo Simulation of Particle Aggregation and Simultaneous Restructuring", *J. Coll. Interf. Sci.*, 213(1999)273
- [20] F. Gruy, "Lois d'évolution de la distribution granulométrique de poudres d'oxydes métalliques calcinées en présence de gaz réactif », *Ann. Chim. Fr* 18(1993)69
- [21] L.L. Tavlarides, M. Stamatoudis, "The analysis of interphase reactions and mass transfer in liquid-liquid dispersions", *Advances in Chem. Eng.* 11(1981)199
- [22] H.R. Kruyt: *Colloid Science*, Elsevier Publishing Company, Amsterdam, 1952
- [23] V. John, I. Angelov, A.A. Öncül, D. Thevenin, "Techniques for the reconstruction of a distribution from a finite number of its moments", *Chem. Eng. Sci.* 62(2007)2890
- [24] S.H. Park, F.E. Kruis, K.W. Lee, H. Fissan, "Evolution of particle size distribution due to turbulent coagulation", *J. Aerosol Sci.*, 31(2000)S572
- [25] S.H. Park, K.W. Lee, "Asymptotic particle size distributions attained during coagulation processes", *J. Coll. Interf. Sci.* 233(2001)117
- [26] S.H. Park, K.W. Lee, "Change in particle size distribution of fractal agglomerates during Brownian coagulation in the free-molecule regime", *J. Coll. Interf. Sci.* 246(2002)85
- [27] F. Gruy, "Méthode approchée pour la reconstruction de la densité de population : cas de l'agrégation-agglomération », *Cristal 6 proceedings*, 99(2010)55, Ed. SFGP, Paris
- [28] F.E. Torres, W.B. Russel, W.R. Schowalter, "Simulations of coagulation in viscous flows", *J. Coll. Interf. Sci.* 145(1991)51
- [29] A.A. Potanin, "On the mechanism of aggregation in the shear flow of suspensions", *J. Coll. Interf. Sci.* 145(1991)140
- [30] M. Smith, T. Matsoukas, „Constant-number Monte Carlo simulation of population balances“, *Chem. Eng. Sci.*, 53(1998)1777
- [31] Y. Adachi, M. Kobayashi, S. Ooi, "Applicability of fractals to the analysis of the projection of small flocs", *J. Coll. Interf. Sci.*, 208(1998)353
- [32] G. Yang, P. Biswas, "Computer simulation of the aggregation and sintering restructuring of fractal-like clusters containing limited numbers of primary particles", *J. Coll. Interf. Sci.*, 211(1999)142
- [33] M. Lattuada, H. Wu, M. Morbidelli, « A simple model for the structure of fractal aggregates » *J. Coll. Interf. Sci.*, 268(2003)106

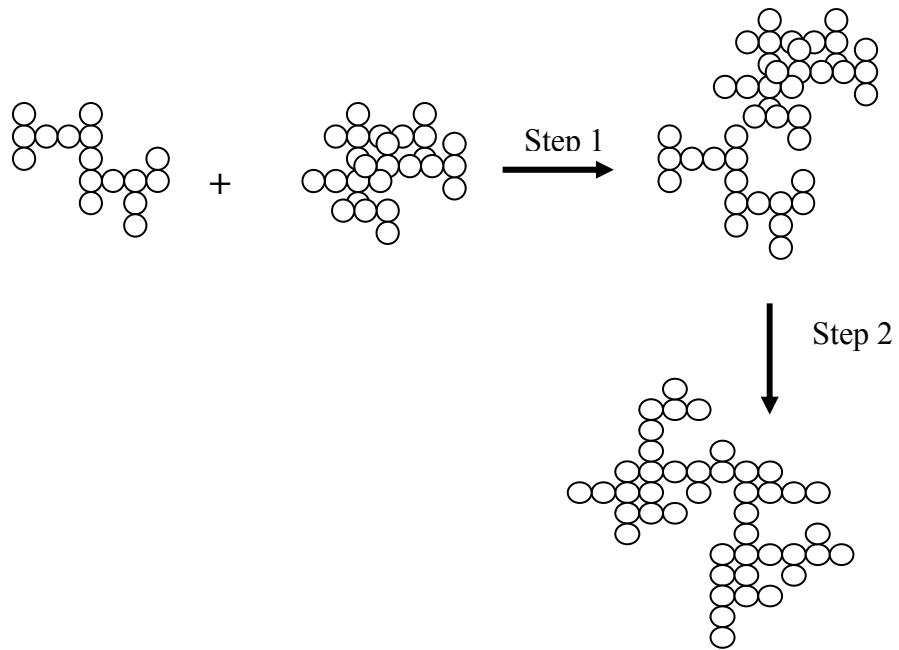
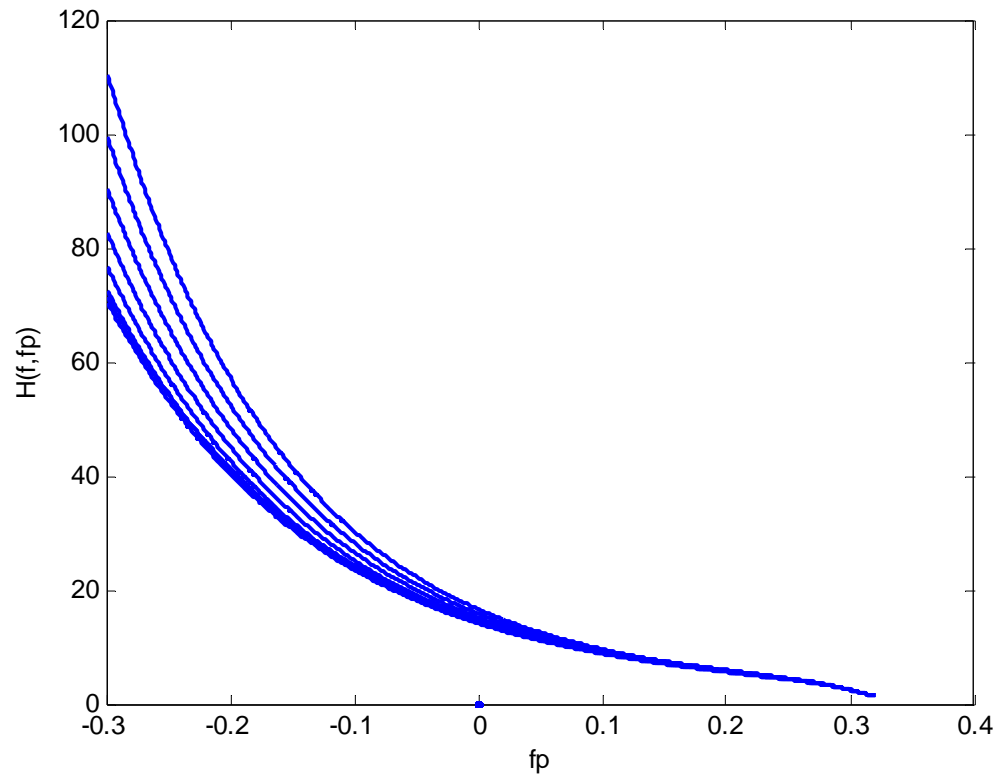


Figure 1: decomposition into two steps in the new formulation of aggregation



$fp=f'$

Figure 2a: $H(f, f')$ is calculated for several f values (from 0.4 to 0.56 by step 0.02), the lowest curve corresponds to $f=0.4$, the highest to $f=0.56$.

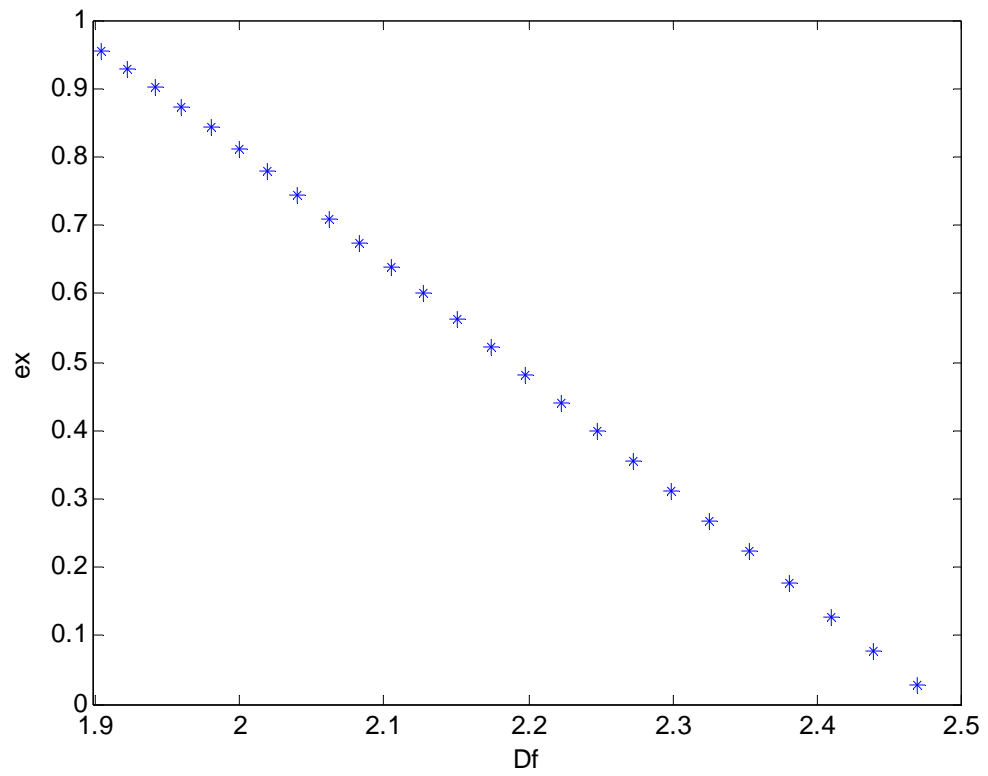


Figure 2b: exponent ex of the power law (Eq. 40c) versus D_f .

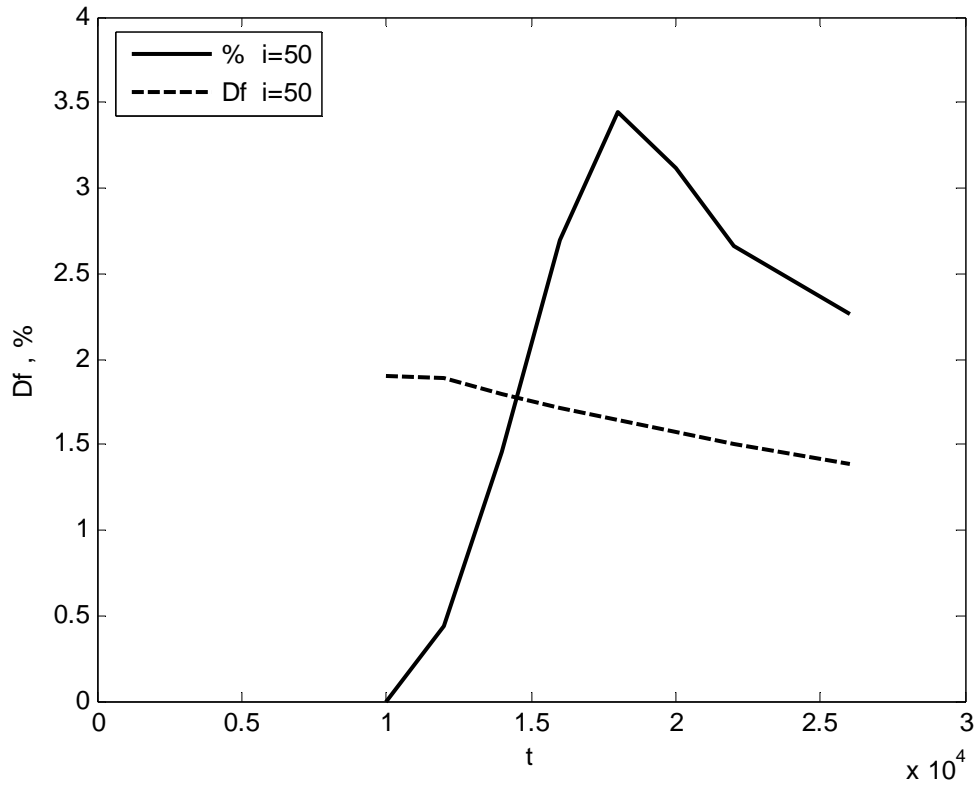


Figure 3: mean fractal dimension and number percentage versus time (time scale following [19]) for $i=50$.

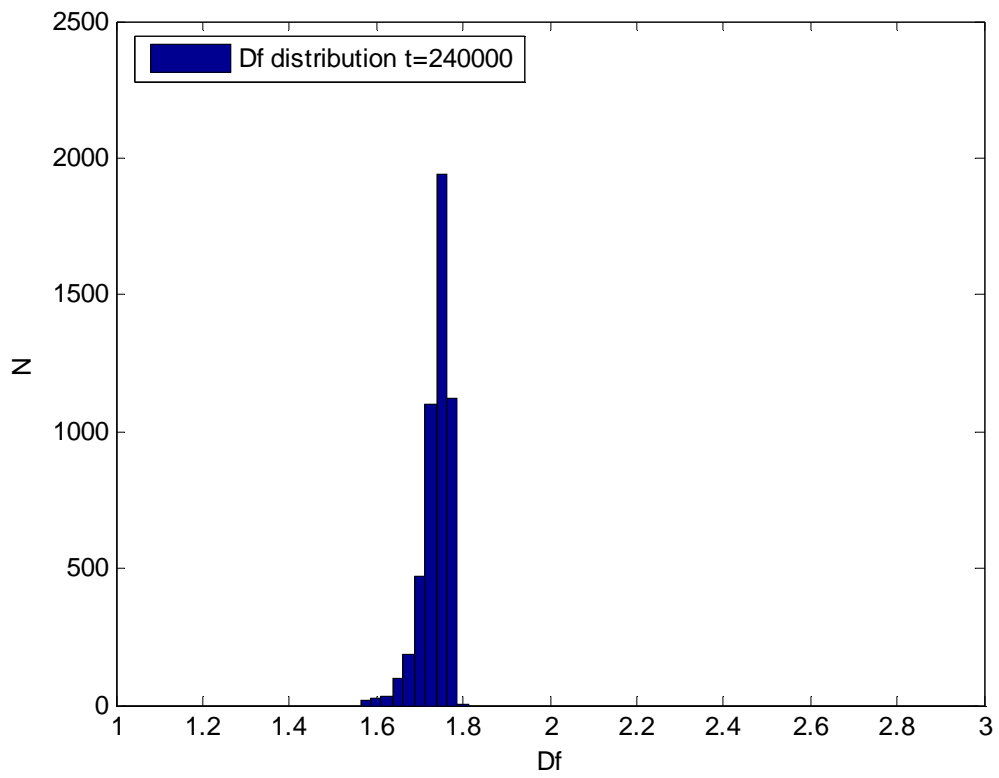


Figure 4: fractal dimension distribution for long time (time scale following [19])